Effectiveness of digital PCR for MYD88[L265P] detection in vitreous fluid for primary central nervous system lymphoma diagnosis

KUN CHEN[1*], YANCHUN MA[1*], TIANLING DING[2], XINJU ZHANG[3], BOBIN CHEN[2] and MING GUAN[1,3]

[1]Department of Laboratory Medicine, Huashan Hospital North, Fudan University; [2]Department of Hematology, Huashan Hospital North, Fudan University, Shanghai 201907; [3]Central Laboratory, Huashan Hospital, Shanghai Medical School, Fudan University, Shanghai 200040, P.R. China

Abstract. Primary central nervous system lymphoma (PCNSL) is a rare type of primary extranodal lymphoma (PEL). MYD88[L265P] mutation has been observed in up to 75% of PCNSL cases, however, the validity and sensitivity of digital PCR in detecting this mutation remains to be elucidated. A total of 44 PCNSL patients, 15 diffuse large B-cell lymphoma not otherwise specified (DLBCL-NOS) patients and 13 other PEL patients were enrolled in the present study. The abilities of reverse transcription quantitative PCR (RT-qPCR) and droplet digital PCR (ddPCR) to detect the MYD88[L265P] mutation in cerebral spinal fluid (CSF) samples were compared. The results suggested that ddPCR showed superior mutation detection sensitivity when compared with RT-qPCR (58 vs. 15%; $P<0.05$). The MYD88[L265P] mutation was significantly associated with increased MYD88 protein overexpression in PCNSL brain tissue samples ($P<0.05$). Analysis of MYD88[L265P] mutation status in CSF and vitreous fluid samples using ddPCR may be a promising technique for minimally invasive confirmation of PCNSL diagnosis.

Introduction

Primary extranodal lymphomas (PELs) are non-Hodgkin's lymphomas that arise in non-lymphatic tissues (1,2). PEL is frequently observed in the gastrointestinal tract and also in the skin, but is seldom seen in the central nervous system (CNS). The tissue of origin of a PEL determines its pathological and molecular features, as well as patient prognosis and therapeutic strategies (3).

Correspondence to: Dr Ming Guan, Central Laboratory, Huashan Hospital, Shanghai Medical School, Fudan University, 12 Wulumuqi Road, Ji'an, Shanghai 200040, P.R. China
E-mail: guanming88@yeah.net

*Contributed equally

Primary central nervous system lymphoma (PCNSL) represents 4% of intracranial tumors and accounts for 4-6% of all reported PELs (4). Patients with CNS-derived PELs usually have a poor prognosis (5,6). Diffuse large B-cell lymphoma (DLBCL) is a common PCNSL sub-type and is usually observed in the brain, eyes, meninges and spinal cord without systemic spread (7). Differential diagnosis of PCNSL is usually achieved by examining a stereotactic brain biopsy or cerebrospinal fluid (CSF) and vitreous fluid (VRF) cytology (if malignancy involves those tissues) (8). However, CSF and VRF cytology is not always feasible, owing to the low yield of tumor cells in the fluid samples (9,10). Therefore other techniques, including immunocytochemistry, determination of cytokine levels, flow cytometry, immunoglobulin gene rearrangement analysis and mutation analysis, are also applied to examine the CSF or VRF (11-13). Nevertheless, the amount of tumor cells in the fluid sampled remains a key determining factor affecting accurate diagnosis (13).

MYD88 (MYD88 innate immune signal transduction adaptor)[L265P] mutation is reported in up to 75% of PCNSL cases and is regarded as a molecular marker for PCNSL (14). In addition, MYD88[L265P] mutation is associated with poor prognosis, especially in elderly patients (15). Therefore, MYD88[L265P] mutation detection in the CSF and/or VRF may be instrumental for the early diagnosis of PCNSL alongside additional diagnostic tools (10,16).

To date, reverse transcription-quantitative PCR (RT-qPCR) and panel next generation sequencing (NGS) are the most commonly used techniques for the detection of MYD88 mutations (13,16). However, samples containing a low concentration of tumor DNA may not reach the threshold (% of the sample containing DNA) required for either technique (NGS, 2-5%; RT-qPCR, ~0.5%) (17). Droplet digital PCR (ddPCR) is a relatively new PCR technique with a superior sensitivity for trace mutation identification compared to conventional PCR techniques (18). In the present study, the feasibility of ddPCR in the diagnostic detection of MYD88[L265P] mutation in lymphomas was examined using both CSF and VRF samples and additional tumor tissue samples.

Materials and methods

Patients. The data from 72 patients that had presented with DLBCL were retrospectively analyzed in the present

study. All patients were examined in the Department of Hematology, Huashan Hospital North between January 2013 and December 2016. A total of 44 cases of PCNSL, 15 cases of DLBCS not otherwise specified (DLBCL-NOS), and 13 cases of other PELs (2 cases in breast, 3 cases in testis, 3 cases in bone, 4 cases in the gastrointestinal tract and 1 case in the mediastinum) were analyzed. A total of 55 formalin-fixed paraffin-embedded (FFPE) brain, lymphatic or malignancy involved tissues were obtained following surgical resection (PCNSL=29, DLBCL-NOS=15 and PEL=11). CSF samples were collected by lumbar puncture from 26 PCNSL and 2 testis-PEL patients. Among them, 18 samples were collected as paired biopsies of the malignant tissues (16 PCNSL and 2 testis-PEL). A total of 25 VRF samples were collected after either single-side (n=9) or double side (n=8) vitrectomy, and among them 5 cases were collected as paired biopsy with the malignant tissues. Further details of patient characteristics can be found in Table I. The protocol of this study was approved by the Huashan Hospital Institution Review Board (HIRB) and informed written consent was obtained from all enrolled patients. The diagnoses of all enrolled patients were reviewed and confirmed according to the diagnostic criteria and classification of the World Health Organization (7).

-qPCR and ddPCR. Genomic DNA was extracted from the FFPE tissue sections using the QIAamp DNA FFPE tissue kit (Qiagen GmBH) and circulating DNA (ctDNA) was extracted from CSF or VRF samples using the QIAamp circulating nucleic acid kit (Qiagen GmBH) according to the manufacturer's instructions. In addition, genomic DNA was extracted from the bone marrow of a lymphoplasmacytic lymphoma patient (positive control for MYD88^{L265P} mutation) or from the VFR DNA obtained from an intraocular infiltrated NK/T-cell lymphoma patient (negative control), using the QIAamp circulating nucleic acid kit according to the manufacturer's instructions. TaqMan probes purchased from Thermo Fisher Scientific, Inc were as follows: MYD88-L265P-CT-T2 (HEX-GCGACTGATCC-BHQ1), and MYD88-L265P-CT-C2 (FAM-GCGACCGATCC-BHQ1).

The extracted DNA was amplified by qPCR on a Roche cobas Z 480 real-time PCR platform (Roche Applied Science) using a Kapa probe fast universal qPCR Kit (Kapa Biosystems; Roche Diagnostics) according to the standard protocols. Primer sequences used for amplification were as follows: MyD88-L265P forward, 5'-CATGGCACCCCTTGGCTT-3' and reverse, 5'-CCTCAGGATGCTGGGGAAC-3'. qPCR was conducted under the following conditions: Initial denaturation at 95°C for 3 min followed by 40 cycles of 95°C for 30 sec, 60°C for 30 sec and 72°C 30 sec, with a final extension at 72°C for 1 min. qPCR data were quantified using $2^{-\Delta\Delta Cq}$ analysis (19). Alternatively, the extracted DNA was amplified by ddPCR on a QX200 ddPCR system (Bio-Rad Laboratories, Inc.) according to manufacturer's instructions and the results were visualized by a QuantaSoft software (version 1.7.4; Bio-Rad Laboratories, Inc.). ddPCR was conducted under the following conditions: Initial denaturation at 95°C for 10 min, followed by 40 cycles of 95°C for 30 sec, 58°C for 30 sec and 72°C for 1 min, with a final extension at 98°C for 10 min. GAPDH (forward: 5'-GGA GCGAGATCCCTCCAAAAT-3', reverse: 5'-GGCTGTTGT CATACTTCTCATGG-3') was used as a loading control.

Each sample was analyzed in duplicate and a positive as well as a negative control sample was included for quality control and to determine the fluorescence thresholds. The primer sequences and fluorescent probes used in the ddPCR procedures were identical to those of qPCR and they were prepared with 2X master-mix solution (Bio-Rad Laboratories, Inc.). For each sample, the reaction wells were clustered into four groups, [wild type (HEX positive), mutant (FAM positive), heterozygote (double positive), and no-template (double negative)], in the fluorescence signal intensity 2D plot. Absolute quantification of each sample was subsequently achieved in copies/µl (molecules DNA/µl) by Poisson's distribution correction. Furthermore, QuantaSoft 1.7.4 software (Bio-Rad Laboratories, Inc.) was used to calculate the fractional abundance (mutation frequency), irrespective of mutant positive droplets amount. Therefore, samples negative for MYD88^{L265P} showed a fractional abundance above 0.0%.

Immunohistochemistry. Following fixation at 4°C at least overnight and paraffin embedding, the FFPE tissues were sectioned at 2 to 4 µm thickness on a microtome. Immunohistochemistry was performed using a Ki67 primary antibody working solution (1:1,000; cat. no. MAB-0672; MXB Biotechnologies) or MyD88 primary antibody solution (1:800; OriGene Technologies, Inc.; cat. no. TA502117) and a REAL EnVision detection system (Dako; Agilent Technologies, Inc.) according to the manufacturer's instructions. Next, the sections were counterstained with hematoxylin and eosin (H&E) at room temperature for 10 min using an H&E staining kit (Baso Diagnostics, Inc.). Slides were independently examined by two experienced pathologists using the microscope Nikon50i (Nikon Corporation) with x400 magnification. The staining was scored semi-quantitatively and recorded based on both the cytoplasmic staining (0=negative, 1=1-25% immunoreactive cells, 2=26-50% immunoreactive cells, 3=51-75% immunoreactive cells, and 4=76-100% immunoreactive cells) as well as the staining intensity (0=negative, 1=weak, 2=moderate and 3=strong). The stainings were manually calculated by two experienced pathologists.

Statistical analysis. The data were presented as means ± SEM. The differences among the clinical characteristics were compared using the χ^2-test or the Fisher's exact test, according to the sample size. All statistical analysis was performed with SPSS (version 21.0; IBM Corp.). P<0.05 was considered to indicate a statistically significant difference.

Results

Demographic characteristics and clinical features of the enrolled patients. Analysis of the demographic characteristics indicated that there was no significant difference in the gender (P=0.082) or median age (P=0.236) among the enrolled patients (Table I). The median age of patients with PCNSL was 59 years (range, 41-72 years). The median age of patients with DLBCL-NOS was 60 years (range, 45-86 years) and for patients with other PELs the median age was 52 years (range, 27-84), whose ages were not significant difference among these groups. When compared with the DLBCL-NOS and PELs patients, the PCNSL patients presented with cranial hypertension and dyskinesia more often (P<0.05), but no B

Table I. Clinical parameters of the enrolled patients.

Clinical feature	PCNSL	DLBCL-NOS	Other PEL
Number of patients	44	15	13
Sex			
Male	22	8	11
Female	22	7	2
Age, years (range)	59 (53.5-64.5)	60 (54.3-72.5)	52 (46.8-64.0)
<60	22	7	8
≥60	22	8	5
Clinical manifestation			
Intracranial hypertension	9	0	0
Movement disorders	26	2	4
Sensory dysfunction	4	0	0
Speech disorders	5	0	0
Visual disturbance	10	0	2
Cognitive disorders	3	0	1
Facioplegia	5	1	0
Convulsion	1	0	0
Tumor tissue (n=55)	29	15	11
Brain tumor tissue	29	0	1
Lymphatic tumor tissue	0	15	0
Other tumor tissue	0	0	10
CSF (n=28)	26	0	2
VRF (n=25)	22	0	3

CSF, cerebrospinal fluid; DLBCL-NOS, diffuse large B-cell lymphoma-not otherwise specified; PCNSL, primary central nervous system lymphoma; PEL, primary extranodal lymphoma; VRF, vitreous fluid.

symptoms (fever, night sweats, or weight loss) were observed (P<0.01). There were no obvious neurological symptoms in the DLBCL-NOS and other PELs patients (P<0.01). However, cranial hypertension, dyscinesia and visual impairment could occur after the CNS was affected (data not shown).

The diagnosis of PCNSL patients (n=44) was evaluated according to the guidelines of the International PCNSL Collaborative Group Report, including by magnetic resonance imaging of the brain, ophthalmologic evaluation and CSF evaluation (13) (Table IV). Imaging results demonstrated that a total of 24 PCNSL patients presented with multifocal lesions (24/44; 54.5%), while the other 20 patients had a single lesion (20/44; 45%). The lesions were mainly located in the front-temporal lobe (35/44; 79.5%) and deep structures (25/44; 56.8%), while the eyes (14/44; 31.8%) were less frequently involved. There was no bone marrow invasion observed among the PCNSL patients; whereas, bone marrow invasion was detected in 6 DLBCL-NOS patients (6/15; 40%). The serum LDH and β2-microglobin concentration was significantly different among the three examined groups (P<0.01). There was no significant difference in the CSF evaluation parameters (pressure, protein concentration or cytology) among the examined groups (P>0.05).

Detection of MYD88^{L265P} in tissue and CSF/VRF using ddPCR. Among the collected lymphoma tissue samples,

28 of the evaluable tissue samples (28/55, 50.9%) harbored the MYD88^{L265P} mutation. In the PCNSL patients (n=44), genomic DNA was extracted from 29 tissue samples, 17 VFR samples and 26 CSF samples. The sensitivity of MYD88^{L265P} mutation detection was similar between qPCR and ddPCR in the case of DNA samples obtained from PCNSL tissues. Using both qPCR and ddPCR, positive MYD88^{L265P} mutation was identified in 72.4% (21/29) PCNSL tissue samples. Compared to qPCR, the sensitivity of mutation detection was significantly higher in ddPCR for CSF/VRF DNA samples (P<0.05). Specifically, conventional qPCR detected positive MYD88^{L265P} mutation in 15.4% (4/26) of the PCNSL CSF samples, while ddPCR could identify MYD88^{L265P} mutation in 57.8% (15/26) of the PCNSL CSF, including the 4 qPCR positive ones (Table II). Meanwhile, qPCR identified MYD88^{L265P} mutation in 70.61% (12/17) of the VRF samples while ddPCR detected an additional positive MYD88^{L265P} mutation (13/17; 76.5%). Interestingly, double side vitrectomy significantly increased the sensitivity of ddPCR-based MYD88^{L265P} mutation detection by 35% (13/17 vs. 7/17 in the single side sample) (P=0.031; P<0.05; Table III).

Among the 18 CSF samples derived from the PEL paired samples, positive MYD88^{L265P} mutation was detected in 9 (50%) sample pairs by ddPCR using Fisher's exact test, which emphasizes the value of paired sampling (Table III). Furthermore, multisite sampling improved the diagnosis

Table II. Immunophenotypic studies and mutational status of MYD88 L265P.

	Positive MYD88 Protein expression ratio	MyD88^L265P mutation using ddPCR		
		Tumor tissue (%)	VRF	CSF
PCNSL	18/29 (62.1%)	21/29 (72.4)	11/15 (73.3%)	15/26 (57.7%)
DLBCL-NOS	0/15 (0.0%)	2/15 (13.3)	NA	NA
Other PEL	5/11 (45.5%)	5/11 (45.5)	2/2 (100%)	1/2 (50%)
Total	NA	28/55 (50.9)	13/17 (76.5%)	16/28 (57.1%)

CSF, cerebrospinal fluid; DLBCL-NOS, diffuse large B-cell lymphoma-not otherwise specified; MYD88, MYD88 innate immune signal transduction adaptor; PCNSL, primary central nervous system lymphoma; PEL, primary extranodal lymphoma; VRF, vitreous fluid.
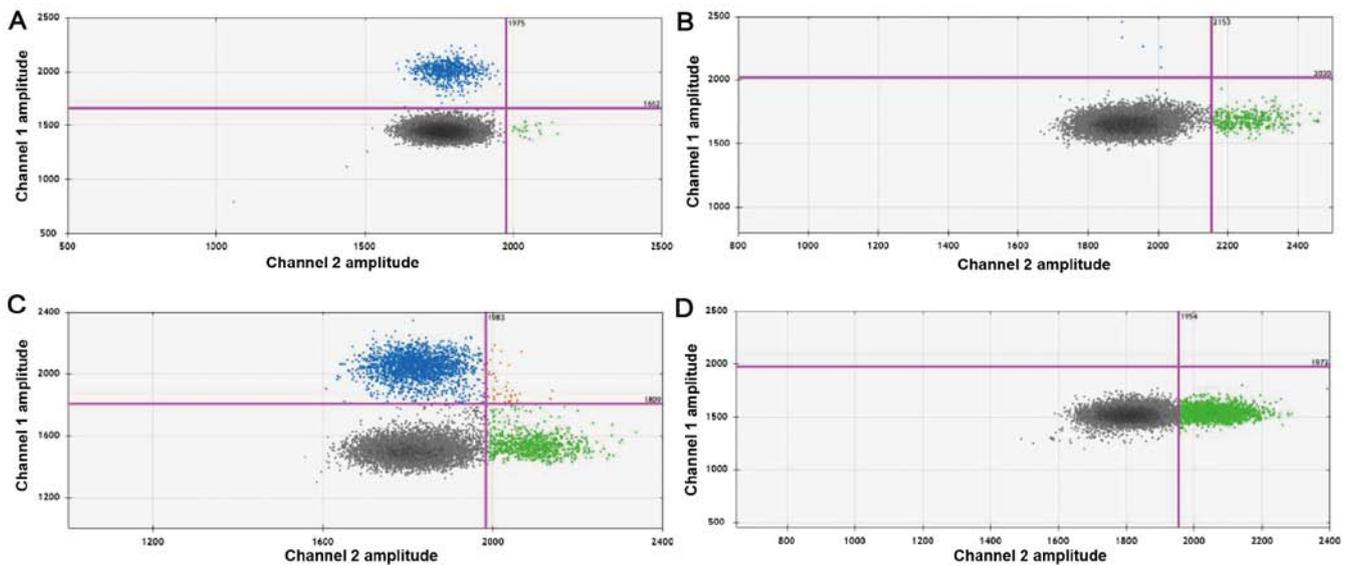

Figure 1. Representative results of ddPCR in the VRF and CSF samples. (A) A positive CSF sample, (B) a negative CSF sample, (C) a positive VRF sample and (D) a negative VRF sample with compact droplet clusters due to DNA quality. The upper left quadrant shows mutant cluster; upper right quadrant shows double positive (both mutant and wild-type template present) cluster; bottom right quadrant shows wild-type cluster; bottom left quadrant shows negative cluster. The purple lines represent the threshold values of the fluorescence intensity. X axis represents the channel 2 of green fluorescent (HEX), and Y axis represents the channel 1 of Carboxyfluorescein (FAM).

efficiency. For instance, in patient 15, the left eye VRF sample was negative in both cytology and mutation analysis, while the CSF sample was identified as MYD88^L265P positive by ddPCR (Fig. 1A).

MYD88^L265P mutation is associated with MYD88 upregulation in PCNSL. Next, the immunophenotypic features of MYD88^L265P mutation among patients in the cohort were investigated (Tables IV and V; Fig. 3). FFPE tissues from PCNSL, DLBCL-NOS and PEL patients were immunostained with anti-MYD88 antibody. There was no positive MYD88 expression in the DLBCL-NOS FFPE tissues (0/15; data not shown). In the PCNSL and PELs tissues, there was no significant difference in MYD88 protein expression (18/29, 62.1% positive protein expression vs. 5/11, 45.5% positive MYD expression, respectively; Table IV; Fig. 3). Interestingly, MYD88^L265P mutation was significantly associated with PCNSL (34/72, 47.2%; $P<0.05$; Table II). The ddPCR analysis demonstrated that 28 of the 55 lymphoma tissue samples (28/55; 50.9%) harbored the MYD88^L265P mutation (Table II). Among them, 21 cases

were from PCNSL patients (21/29; 72.4%), 2 cases were from DLBCL-NOS patients (2/15; 13.3%) and 5 samples were obtained from other-PEL patients (5/11; 45.5%). Therefore, positive MYD88^L265P mutation was significantly more prevalent in PCNSL samples ($P<0.001$; Table II). In the present study cohort (n=72), the PEL tissue of origin included the brain, eye, CSF and other extranodal and lymph nodals. However, brain tissue showed the highest MYD88^L265P mutational rate (21/30, 70%), followed by VRF (20/25; 80.0%), and CSF samples (15/28; 53.6%; Fig. 2). In PCNSL patients, MYD88^L265P mutation in brain tissues was significantly associated with MYD88 protein upregulation (r=0.421, P=0.038; Table V). Moreover, the presence of positive MYD88^L265P mutation was observed in up to 40.9% (9/22) of the CSF samples if the brain tissue was positive for the same mutation (Fig. 4).

Discussion

PCNSLs are primary lymphomas of the CNS that include DLBCL and other rare lymphomas, for example T-cell

Table III. MYD88 L265P mutation detection by ddPCR in CSF and vitreous fluid samples.

Sample	Tissue	MYD88^L265P CSF	VRF L	VRF R
1	Mut	WT (0.00)	NA	NA
2	Mut	WT (0.07)	NA	NA
3	Mut	WT (0.05)	NA	NA
4	Mut	WT (0.00)	NA	NA
5	Mut	WT (0.00)	NA	NA
6	Mut	WT (0.00)	NA	NA
7	Mut	Mut (1.10)	NA	NA
8	Mut	Mut (1.80)	NA	NA
9	Mut	Mut (0.92)	NA	NA
10	Mut	Mut (3.10)	NA	NA
11	Mut	Mut (1.20)	NA	NA
12	Mut	Mut (1.03)	NA	NA
13	Mut	Mut (1.10)	Mut (5.40)	NA
14	Mut	Mut (0.90)	Mut (3.80)	NA
15	Mut	Mut (44.3)	WT (0.08)	NA
16	Mut	WT (0.00)	Mut (10.70)	NA
17	Mut	WT (0.00)	Mut (7.70)	Mut (1.90)
18	Mut	WT (0.00)	Mut (12.30)	Mut (11.30)
19	NA	WT (0.00)	Mut (0.83)	NA
20	NA	WT (0.00)	Mut (6.30)	Mut (2.2)
21	NA	WT (0.00)	Mut (5.00)	Mut (0.99)
22	NA	WT (0.00)	Mut (0.83)	Mut (5.00)
23	NA	Mut (2.60)	NA	Mut (13.00)
24	NA	Mut (0.63)	NA	NA
25	NA	Mut (0.92)	NA	NA
26	NA	Mut (0.62)	NA	NA
27	NA	Mut (1.20)	NA	NA
28	NA	Mut (0.82)	NA	NA

CSF, cerebrospinal fluid; VRF, vitreous fluid; L, left eye; R, right eye; WT, wild type Mut, mutation; NA, not available.
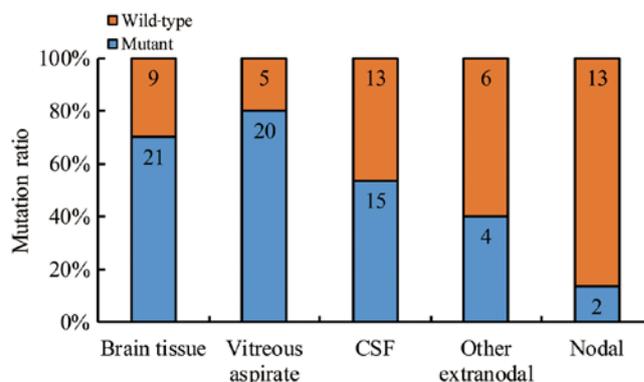

Figure 2. Frequency of MYD88^L265P mutation in 72 DLBCL tissues. DLBCL, diffuse large B-cell lymphoma; MYD88, MYD88 innate immune signal transduction adaptor.
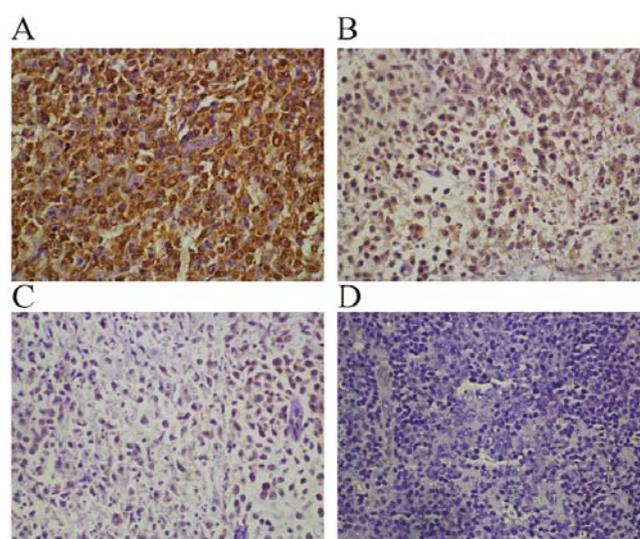

Figure 3. Representative MYD88 protein expression in PCNSL brain tissues. Sections were immunostained with anti-MYD88 antibody, and semi-quantitatively scored according to the staining intensity. Representative images of MYD88-positive brain PCNSL tissue. (A) Strong, 90-100% immunoreactive cells. (B) Moderate, 50-70% immunoreactive cells. (C) Weak, 30-50% immunoreactive cells. (D) MYD88-negative brain PCNSL tissue. Magnification, x40. MYD88, MYD88 innate immune signal transduction adaptor; PCNSL, primary central nervous system lymphoma.

lymphoma and Burkitt lymphoma. The incidence of PCNSL increases with age, with an estimated median age of onset between 55 and 65 years old (20). The etiology of PCNSL remains to be elucidated, but Epstein-Barr or human immunodeficiency virus infection, organ transplantation and immunodeficiency have been reported to be major contributors to development of the disease (17,21). Löw et al (22), previously reported that administering a high methotrexate dose could lead to a high treatment response rate in PCNSL patients. However, the relapse rate can reach up to 50% with the 5-year survival rate ranging from 22-40% (23,24). In PCNSL, MYD88^L265P is a hot-spot mutation, which alters interleukin-1 and toll-like receptor signaling and leads to the hyperactivation of the NF-κB (25) and JAK/STAT signaling pathways (26-28). This mutation can be found in extranodal DLBCL in tissues including the testis, CNS, breast and skin (14, 29-32). In PCNSL, a number of studies have demonstrated that the rate of MYD88^L265P mutation ranges from 73-94.4% (10,14,16,29-31). Interestingly, MYD88^L265P mutation has not been detected in other CNS tumors, for example glioblastoma (33). Therefore, accurate identification of the MYD88^L265P mutation may be a critical step for PCNSL diagnosis.

Identification of circulating tumor cells and circulating tumor DNA in peripheral fluids has become instrumental for the micro-invasive diagnosis of tumors (34). Previous studies reported that MYD88^L265P detection in the CSF using NGS or qPCR may be a powerful tool for disease diagnosis (16,35-37). In the present study, the diagnostic value of ddPCR in detecting the MYD88^L265P mutation in PCNSL VRF, CSF and FFPE samples was validated.

Table IV. Clinical imaging performance and clinicopathological features.

Parameter	PCNSL	DLBCL-NOS	Other PEL	P-value
Number of patients	44	15	13	
Lesion location				
Front-temporal lobe	35	0	1	<0.001
Deep structures	25	0	3	<0.001
Eyes	14	0	2	0.030
Lesion Number				
Multiple	24	0	2	<0.001
Single	20	0	2	
Involvement of bone marrow	0	6	3	<0.001
LDH elevated[a]	5	7	3	0.007
Serum β2-M elevated[b]	11	11	4	0.001
CSF pressure[c]	6	NA	0	0.281
High CSF protein level[d]	12	NA	1	0.176
Abnormal CSF cytology	10	NA	2	0.664

[a]The case number whose LDH over 250 mmol/l; [b]The case number whose β2-M over 2.2 mg/l; [c]The case number whose pressure of CSF over 80 mm H2O; [d]CSF protein concentration over 45 mg/dl in patients ≤60 years old and 60 mg/dl in patients >60 years old. PCNSL, primary central nervous system lymphoma; DLBCL-NOS, diffuse large B-cell lymphoma-not otherwise specified; PEL, primary extranodal lymphoma; LDH, lactate dehydrogenase; β2-M, β2-microglobulin; CSF, cerebrospinal fluid; NA, not available.

Table V. Relationship between MYD88 protein and MYD88[L265P] mutation in PCNSL.

MYD88 Protein	MYD88[L265P]		
	Mut	WT	Total
Negative	6	5	11
Low	5	2	
Medium	2	0	
Positive			18
High	5	1	
Very high	3	0	
Total	21	8	29

Mut, mutation; WT, wild type.

Figure 4. Mutation rate of MYD88 [L265P] in PCNSL brain and CSF samples. CSF, cerebrospinal fluid; MYD88, MYD88 innate immune signal transduction adaptor; PCNSL, primary central nervous system lymphoma.

In the present study patient cohort, the mutation rate of MYD88[L265P] in PCNSL was 77.2% (34/44), which came in agreement with the reported rates in Caucasians (33.3-38%) (38,39) and East Asian patients (63.6-85.4%) (15,30,40). The MYD88[L265P] mutation was more frequently observed in the CNS than in the lymph nodes (70% in brain tissues, 80% in vitreous bodies and 53.6% in CSF). This phenomenon can be attributed to the anatomical structure of the immune barrier in the tissue of origin, such as the CNS, eyes and testicles (29). MYD88[L265P] mutation activates the toll-like receptor/MYD88 signal, which can lead to the selective growth of lymphoma cells in this particular immune region (41). The results of the present study indicated an association between MYD88[L265P] mutation and increased MYD88 protein expression in PCNSL
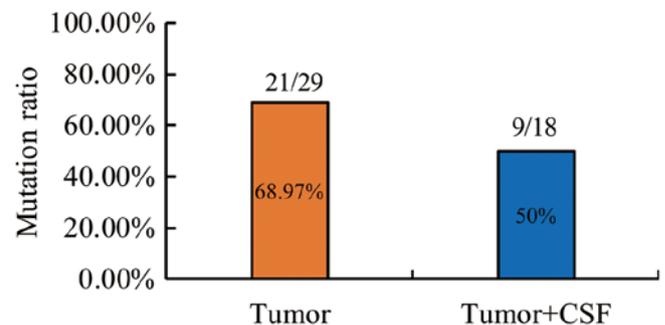
tissues, thereby, providing further evidence to support the abovementioned hypothesis.

To date, NGS and qPCR are the most popular techniques for the detection of MYD88[L265P] mutation. However, the high cost of NGS hinders its wide-scale use for diagnostic purposes (42). The results of the present study indicated that the RT-qPCR detection sensitivity for MYD88[L265P] mutation in the CSF was only 14.3% (4/28). This could possibly be attributed to a low level of tumor DNA in the CSF, which hampered the amplification process. On the other hand, the sensitivity of MYD88[L265P] mutation detection was 54.6% (15/28) using ddPCR, which was a significantly higher rate of MYD88[L265P] mutation in CSF compared with that previously reported (31%) (43). The diagnosis of intraocular lymphoma, when lymphoma cells invade the eye tissues, can sometimes be challenging (44,45); therefore, vitreous cell pathology through vitrectomy may be a new gold standard for disease diagnosis. Using ddPCR,

MYD88^{L265P} mutation detection was successfully achieved in 76% (13/17) of the highVRF samples; whereas, using qPCR 71% (12/17) of MYD88^{L265P} mutations were detected. These findings suggested that VRF may be a valuable micro-invasive sample for the molecular diagnosis of VRL. Presently, at the early stages of PCNSL, CSF is sufficient for diagnosis in clinic. With progression of the disease, PCNSL may affect the eyes in 15-25% patients, which must be confirmed by VRF analysis (46). VRF analysis may contribute to improving the sensitivity of vitreoretinal lymphoma diagnosis. Additionally, MYD88^{L265P} mutation displays 100% specificity for diagnosis in VRF.

PCNSL is a relatively rare intracranial tumor. At present, its diagnosis is accomplished via intracranial biopsy or CSF/VRF cytological pathology. CSF/VRF cytology requires the presence of intact tumor cells in the sample. Consequently, a high rate of false negative results is usually observed when the number of tumor cells is low in the CSF/VFR. In addition, treatment with chemotherapy and steroids may negatively impact the number of intact tumor cells in the CSF/VRF (47). These shortcomings can be overcome by the analysis of circulating tumor DNA in CSF/VRF samples. Therefore, detection of circulating tumor DNA may be a promising methodology for the diagnosis of CNS lymphoma.

ddPCR has been determined to be the most sensitive method to detect MYD88^{L265P} in ctDNA of bone marrow or peripheral blood in cases of Waldenstrom macroglobulinemia (16,34). In the present study, patient 12 was a noteworthy case. This 60-year old female was diagnosed with lymphoplasmacytic lymphoma in December 2016. Her symptoms were headache, abnormal sensation and dyskinesia. MRI showed that the left frontal lobe was occupied by lesions. MYD88^{L265P} mutation was detected in both her bone marrow and her CSF. Her condition was confirmed to be Bing-Neel syndrome (BNS), a rare manifestation of Waldenstrom's macroglobulinemia that results from infiltration of the central nervous system by malignant lymphoplasmacytic cells (48). It was puzzling that a large number of tumor cells were found in the CSF of this patient, which presented with morphology different to lymphoplasmacytic cells and closer to the morphology of DLBCL cells. A surgical biopsy of the patient was performed. The histopathological diagnosis was DLBCL, and MYD88^{L265P} mutation was also detected. However, the immunohistochemical staining of the tissue did not indicate evidence of infiltration of lymphoplasmacytic cells. The immunoglobulin heavy chain (IGH) rearrangement between brain and bone marrow tissue was then assessed. According to the results of IGH rearrangement and histopathological type, it could be concluded that the patient had two distinct types of tumors. From this case, it can be concluded that BNS or PCNSL cannot be diagnosed only by the detection of MYD88^{L265P} mutation in the CSF, which should only be used as an indicator of auxiliary diagnosis.

In conclusion, MYD88^{L265P} mutation is a valuable marker for PCNSL diagnosis. Detection of the mutation in the CSF and VRF samples by ddPCR is a promising micro-invasive tool to confirm the PCNSL diagnosis or exclude other CNS malignancies. However, the combination of various molecular techniques with conventional CSF/VRF cytology should be encouraged to improve diagnostic specificity and sensitivity.

Availability of data and materials

The datasets used and/or analyzed during the present study are available from the corresponding author on reasonable request

Authors' contributions

KC, MG and BC designed the study. KC, YM and XZ performed the experiments. KC and TD analyzed the data. KC and YM drafted and revised the manuscript. All authors read and approved the final version of the manuscript.

Ethics approval and consent to participate

The protocol of the current study was approved by the Huashan Hospital Institution Review Board (HIRB) and informed written consent was obtained from all enrolled patients.

Patient consent for publication

Not applicable.

Competing interests

The authors declare that they have no competing interests.

References

1. Oh MY, Oh SB, Seoung HG, et al.: Clinical significance of standardized uptake value and maximum tumor diameter in patients with primary extranodal diffuse large B cell lymphoma. The Korean journal of hematology 47: 207-212, 2012.
2. Kashyap R, Rai Mittal B, Manohar K, et al.: Extranodal manifestations of lymphoma on [(1)(8)F]FDG-PET/CT: a pictorial essay. Cancer imaging : the official publication of the International Cancer Imaging Society 11: 166-174, 2011.
3. Illerhaus G, Schorb E and Kasenda B: Novel agents for primary central nervous system lymphoma: evidence and perspectives. Blood 132: 681-688, 2018.
4. Ferreri AJ: How I treat primary CNS lymphoma. Blood 118: 510-522, 2011.
5. Shi Y, Han Y, Yang J, et al.: Clinical features and outcomes of diffuse large B-cell lymphoma based on nodal or extranodal primary sites of origin: Analysis of 1,085 WHO classified cases in a single institution in China. Chinese journal of cancer research = Chung-kuo yen cheng yen chiu 31: 152-161, 2019.
6. Ferreri AJ: Risk of CNS dissemination in extranodal lymphomas. Lancet Oncol 15: e159-169, 2014.
7. Sabattini E, Bacci F, Sagramoso C and Pileri SA: WHO classification of tumours of haematopoietic and lymphoid tissues in 2008: an overview. Pathologica 102: 83-87, 2010.
8. Hoang-Xuan K, Bessell E, Bromberg J, et al.: Diagnosis and treatment of primary CNS lymphoma in immunocompetent patients: guidelines from the European Association for Neuro-Oncology. Lancet Oncol 16: e322-332, 2015.

9. Cesana C, Klersy C, Scarpati B, et al.: Flow cytometry and cytomorphology evaluation of hematologic malignancy in cerebrospinal fluids: comparison with retrospective clinical outcome. Ann Hematol 90: 827-835, 2011.

10. Raja H, Salomao DR, Viswanatha DS and Pulido JS: Prevalence Of Myd88 L265p Mutation In Histologically Proven, Diffuse Large B-Cell Vitreoretinal Lymphoma. Retina 36: 624-628, 2016.

11. Araujo I and Coupland SE: Primary Vitreoretinal Lymphoma -- A Review. Asia-Pacific journal of ophthalmology 6: 283-289, 2017.

12. Shin SY, Lee ST, Kim HJ, et al.: Usefulness of Flow Cytometric Analysis for Detecting Leptomeningeal Diseases in Non-Hodgkin Lymphoma. Annals of laboratory medicine 36: 209-214, 2016.

13. Liu L, Cao F, Wang S, Zhou J, Yang G and Wang C: Detection of malignant B lymphocytes by PCR clonality assay using direct lysis of cerebrospinal fluid and low volume specimens. International journal of laboratory hematology 37: 165-173, 2015.

14. Taniguchi K, Takata K, Chuang SS, et al.: Frequent MYD88 L265P and CD79B Mutations in Primary Breast Diffuse Large B-Cell Lymphoma. Am J Surg Pathol 40: 324-334, 2016.

15. Zhou Y, Liu W, Xu Z, et al.: Analysis of Genomic Alteration in Primary Central Nervous System Lymphoma and the Expression of Some Related Genes. Neoplasia 20: 1059-1069, 2018.

16. Hiemcke-Jiwa LS, Minnema MC, Radersma-van Loon JH, et al.: The use of droplet digital PCR in liquid biopsies: A highly sensitive technique for MYD88 p.(L265P) detection in cerebrospinal fluid. Hematol. Oncol. 36: 429-435, 2018.

17. Besson C, Goubar A, Gabarre J, et al.: Changes in AIDS-related lymphoma since the era of highly active antiretroviral therapy. Blood 98: 2339-2344, 2001.

18. Postel M, Roosen A, Laurent-Puig P, Taly V and Wang-Renault SF: Droplet-based digital PCR and next generation sequencing for monitoring circulating tumor DNA: a cancer diagnostic perspective. Expert review of molecular diagnostics 18: 7-17, 2018.

19. Livak KJ and Schmittgen TD: Analysis of relative gene expression data using real-time quantitative PCR and the 2(-Delta Delta C(T)) Method. Methods 25: 402-408, 2001.

20. Olson JE, Janney CA, Rao RD, et al.: The continuing increase in the incidence of primary central nervous system non-Hodgkin lymphoma: a surveillance, epidemiology, and end results analysis. Cancer 95: 1504-1510, 2002.

21. Shiels MS, Pfeiffer RM, Besson C, et al.: Trends in primary central nervous system lymphoma incidence and survival in the U.S. Br J Haematol 174: 417-424, 2016.

22. Low S, Han CH and Batchelor TT: Primary central nervous system lymphoma. Therapeutic advances in neurological disorders 11: 1756286418793562, 2018.

23. Yamanaka R, Morii K, Shinbo Y, et al.: Late relapse of primary central nervous system lymphoma. Leuk Lymphoma 58: 475-477, 2017.

24. Perkins A and Liu G: Primary Brain Tumors in Adults: Diagnosis and Treatment. Am. Fam. Physician 93: 211-217, 2016.

25. Dubois S, Viailly PJ, Bohers E, et al.: Biological and Clinical Relevance of Associated Genomic Alterations in MYD88 L265P and non-L265P-Mutated Diffuse Large B-Cell Lymphoma: Analysis of 361 Cases. Clin Cancer Res 23: 2232-2244, 2017.

26. Xu Y, Li J, Ouyang J, et al.: Prognostic relevance of protein expression, clinical factors, and MYD88 mutation in primary bone lymphoma. Oncotarget 8: 65609-65619, 2017.

27. Ansell SM, Hodge LS, Secreto FJ, et al.: Activation of TAK1 by MYD88 L265P drives malignant B-cell Growth in non-Hodgkin lymphoma. Blood cancer journal 4: e183, 2014.

28. Wenzl K, Manske MK, Sarangi V, et al.: Loss of TNFAIP3 enhances MYD88L265P-driven signaling in non-Hodgkin lymphoma. Blood cancer journal 8: 97, 2018.

29. Kraan W, Horlings HM, van Keimpema M, et al.: High prevalence of oncogenic MYD88 and CD79B mutations in diffuse large B-cell lymphomas presenting at immune-privileged sites. Blood cancer journal 3: e139, 2013.

30. Kraan W, van Keimpema M, Horlings HM, et al.: High prevalence of oncogenic MYD88 and CD79B mutations in primary testicular diffuse large B-cell lymphoma. Leukemia 28: 719-720, 2014.

31. Yamada S, Ishida Y, Matsuno A and Yamazaki K: Primary diffuse large B-cell lymphomas of central nervous system exhibit remarkably high prevalence of oncogenic MYD88 and CD79B mutations. Leuk Lymphoma 56: 2141-2145, 2015.

32. Ngo VN, Young RM, Schmitz R, et al.: Oncogenically active MYD88 mutations in human lymphoma. Nature 470: 115-119, 2011.

33. Fontanilles M, Marguet F, Bohers E, et al.: Non-invasive detection of somatic mutations using next-generation sequencing in primary central nervous system lymphoma. Oncotarget 8: 48157-48168, 2017.

34. Drandi D, Genuardi E, Dogliotti I, et al.: Highly sensitive MYD88(L265P) mutation detection by droplet digital polymerase chain reaction in Waldenstrom macroglobulinemia. Haematologica 103: 1029-1037, 2018.

35. Zorofchian S, Lu G, Zhu JJ, et al.: Detection of the MYD88 p.L265P Mutation in the CSF of a Patient With Secondary Central Nervous System Lymphoma. Front Oncol 8: 382, 2018.

36. Hiemcke-Jiwa LS, Leguit RJ, Snijders TJ, et al.: Molecular analysis in liquid biopsies for diagnostics of primary central nervous system lymphoma: Review of literature and future opportunities. Crit Rev Oncol Hematol 127: 56-65, 2018.

37. Hattori K, Sakata-Yanagimoto M, Suehara Y, et al.: Clinical significance of disease-specific MYD88 mutations in circulating DNA in primary central nervous system lymphoma. Cancer Sci 109: 225-230, 2018.

38. Zorofchian S, El-Achi H, Yan Y, Esquenazi Y and Ballester LY: Characterization of genomic alterations in primary central nervous system lymphomas. J Neurooncol 140: 509-517, 2018.

39. Gonzalez-Aguilar A, Idbaih A, Boisselier B, et al.: Recurrent mutations of MYD88 and TBL1XR1 in primary central nervous system lymphomas. Clin Cancer Res 18: 5203-5211, 2012.

40. Fukumura K, Kawazu M, Kojima S, et al.: Genomic characterization of primary central nervous system lymphoma. Acta Neuropathol 131: 865-875, 2016.

41. Glass S, Phan A, Williams JN, Flowers CR and Koff JL: Integrating understanding of epidemiology and genomics in B-cell non-Hodgkin lymphoma as a pathway to novel management strategies. Discov Med 21: 181-188, 2016.

42. Ding PN, Becker T, Bray V, et al.: Plasma next generation sequencing and droplet digital PCR-based detection of epidermal growth factor receptor (EGFR) mutations in patients with advanced lung cancer treated with subsequent-line osimertinib. Thoracic cancer 10: 1879-1884, 2019.

43. Hiemcke-Jiwa LS, Leguit RJ, Snijders TJ, et al.: MYD88 p.(L265P) detection on cell-free DNA in liquid biopsies of patients with primary central nervous system lymphoma. Br J Haematol 185: 974-977, 2019.

44. Takhar JS, Doan TA and Gonzales JA: Primary vitreoretinal lymphoma: empowering our clinical suspicion. Curr. Opin. Ophthalmol. 30: 491-499, 2019.

45. Lai J, Chen K, Shi HM, et al.: B-scan ultrasound and cytology of the vitreous in primary central nervous system lymphoma with vitreoretinal involvement. Int J Ophthalmol 12: 1001-1007, 2019.

46. Chan CC, Rubenstein JL, Coupland SE, et al.: Primary vitreoretinal lymphoma: a report from an International Primary Central Nervous System Lymphoma Collaborative Group symposium. Oncologist 16: 1589-1599, 2011.

47. Morell AA, Shah AH, Cavallo C, et al.: Diagnosis of primary central nervous system lymphoma: a systematic review of the utility of CSF screening and the role of early brain biopsy. Neuro-oncology practice 6: 415-423, 2019.

48. Kopinska AJ, Helbig G, Koclega A and Kyrcz-Krzemien S: Bing-Neel Syndrome with Detectable MYD88 L265P Gene Mutation as a Late Relapse Following Autologous Hematopoietic Stem Cell Transplantation for Waldenstrom's Macroglobulinemia. Turkish journal of haematology: official journal of Turkish Society of Haematology 34: 186-187, 2017.